ERDC/CHL CHETN-III-78
May 2008

US Army Corps of Engineers®

Estimation of Combined Wave and Storm Surge Overtopping at Earthen Levees

by Steven A. Hughes

PURPOSE: This Coastal and Hydraulics Engineering Technical Note (CHETN) provides empirical equations for estimating several parameters of unsteady flow resulting from the combination of steady storm surge overflow and overtopping of irregular waves at a trapezoidal-shaped earthen levee. Equations are given for the average overtopping discharge and the cumulative probability distribution of instantaneous overtopping discharge. On the landward-side slope, empirical equations can be used to estimate the mean flow depth, mean flow velocity, root-mean-square wave height, and velocity associated with the overtopping wave front. Worked examples illustrate application of the empirical equations.

INTRODUCTION AND BACKGROUND: Earthen levees are used extensively in the United States to protect populations and infrastructure from periodic floods and high water due to storm surges. Overtopping of levees and dikes produces fast-flowing, turbulent water velocities on the landward-side slope that can damage the protective grass covering and expose the underlying soil to erosion. If overtopping continues long enough, the erosion may eventually result in loss of levee crest elevation and perhaps breaching of the protective structure.

Economics often dictate levee designs with crown elevations having a risk that some wave/surge overtopping will occur during extreme events. In addition, crown elevations for older levee systems may have been established without complete information about possible water levels that might occur during extreme events. Even levees that presently have sufficient freeboard to withstand all but the most extreme storms may become vulnerable to wave overtopping and storm surge overflow in the future if sea level continues to rise at projected rates. The cost and engineering challenges of raising all levees to elevations where overtopping will be within tolerable limits may be insurmountable. Levees that cannot be raised remain vulnerable, and the landward-side levee slopes must be protected with some type of strengthening alternative such as turf reinforcement, soil strengthening, or hard armoring.

Assessment of levee reliability and design of slope protection alternatives requires estimates of wave overtopping and storm surge overflow that will occur for a specified set of storm parameters. This CHETN provides overtopping estimation equations for the case of steady overflow due to a still water level above the levee crown elevation combined with irregular wave overtopping. The overtopping flow is unsteady in time and spatially nonuniform, as illustrated in Figure 1. As each overtopping wave passes over the levee crown, it has a somewhat triangular-shaped discharge distribution with a maximum discharge at the leading edge that is several times greater than the time-averaged discharge. If the storm surge elevation above the levee crown is small and/or the waves are large, the levee crown and landward-side slope will “go dry” during wave troughs. This fluctuating discharge may contribute to accelerated erosion of the landward-side levee slope.

Report Documentation Page

Form Approved
OMB No. 0704-0188

1. REPORT DATE	2. REPORT TYPE	3. DATES COVERED
MAY 2008		**00-00-2008 to 00-00-2008**

4. TITLE AND SUBTITLE	5a. CONTRACT NUMBER
Estimation of Combined Wave and Storm Surge Overtopping at Earthen Levees	5b. GRANT NUMBER
	5c. PROGRAM ELEMENT NUMBER
6. AUTHOR(S)	5d. PROJECT NUMBER
	5e. TASK NUMBER
	5f. WORK UNIT NUMBER
7. PERFORMING ORGANIZATION NAME(S) AND ADDRESS(ES) **U.S. Army Engineer Research and Development Center,Coastal and Hydraulics Laboratory,3909 Halls Ferry Road,Vicksburg,MS,39180-6199**	8. PERFORMING ORGANIZATION REPORT NUMBER
9. SPONSORING/MONITORING AGENCY NAME(S) AND ADDRESS(ES)	10. SPONSOR/MONITOR'S ACRONYM(S)
	11. SPONSOR/MONITOR'S REPORT NUMBER(S)

12. DISTRIBUTION/AVAILABILITY STATEMENT
Approved for public release; distribution unlimited

13. SUPPLEMENTARY NOTES

14. ABSTRACT

15. SUBJECT TERMS

16. SECURITY CLASSIFICATION OF:			17. LIMITATION OF ABSTRACT	18. NUMBER OF PAGES	19a. NAME OF RESPONSIBLE PERSON
a. REPORT **unclassified**	b. ABSTRACT **unclassified**	c. THIS PAGE **unclassified**	**Same as Report (SAR)**	**142**	

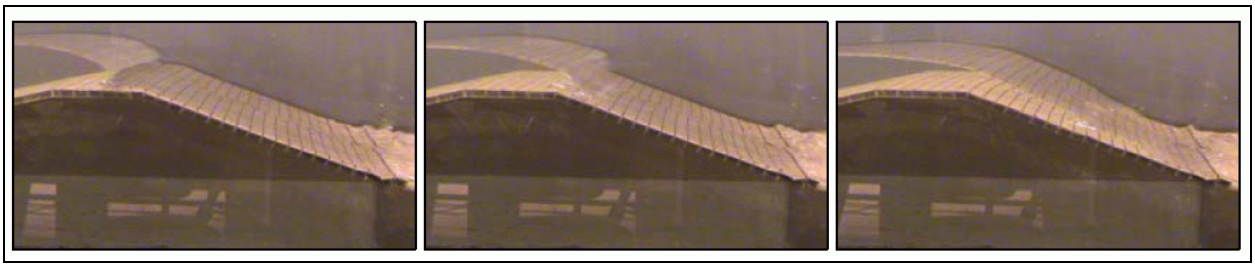

Figure 1. Sequence of wave overtopping on a scale-model levee.

LABORATORY EXPERIMENTS: Laboratory experiments of wave overtopping combined with steady surge overflow were conducted at a nominal prototype-to-model length scale of 25-to-1 in a 3-ft-wide wave flume at the U.S. Army Engineer Research and Development Center's Coastal and Hydraulics Laboratory. The tested levee cross section replicated in the physical model is shown in Figure 2. Seaward is on the left side of the figure, and the dimensions correspond to full-scale units. This cross section was typical of the Mississippi River Gulf Outlet that experienced severe overtopping during Hurricane Katrina.

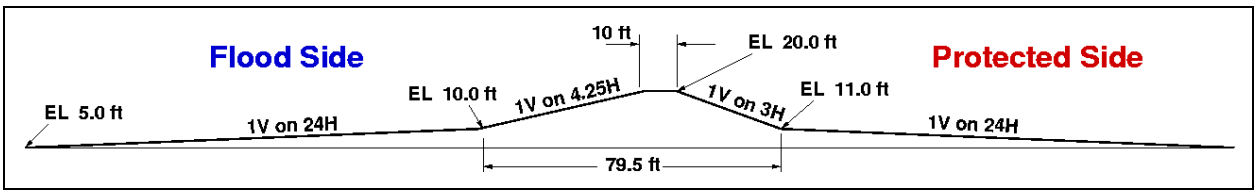

Figure 2. Levee cross section tested in physical model (full-scale dimensions).

Prototype-scale target wave and surge parameters for testing were three surge elevations (S = +1.0, +3.0, and +5.0 ft above levee crest), three significant wave heights (H_{m0} = 3.0, 6.0, and 9.0 ft), and three peak wave periods (T_p = 6, 10, and 14 sec). This gave a total of 27 unique conditions for combined wave and surge overtopping.

Instantaneous discharge over the levee crest was estimated at a location near the landward-side edge of the levee crest. Coincident values of water depth (measured with a pressure gauge) and horizontal velocity (measured with a laser Doppler velocimeter) were multiplied at each instant in time to determine the time series of instantaneous discharge. This estimate assumed that velocity was horizontal and constant throughout the water column at that location. Incident wave characteristics were measured at a three-gauge array located seaward of the levee.

For overtopping, the freeboard is defined as the difference between the levee crest elevation, h_c, and the still-water elevation, h_S, i.e., $R_c = (h_c - h_S)$. When the water elevation is higher than the levee crest, $R_c < 0$, which is referred to as *negative freeboard*.

AVERAGE DISCHARGE FOR COMBINED WAVE AND SURGE OVERTOPPING: For each of the 27 experiments, an average was calculated over the portion of the instantaneous discharge time series that included both wave overtopping and steady overflow. This average represents the average overtopping discharge for that particular combination of negative freeboard

and incident irregular waves. It is customary in overtopping research to express the average wave overtopping discharge in terms of a dimensionless parameter defined as

$$Q_{ws} = \frac{q_{ws}}{\sqrt{g\ H_{m0}^3}} \tag{1}$$

where

Q_{ws} = dimensionless average discharge due to combined waves and surge
q_{ws} = average discharge due to combined waves and surge per unit crest length
g = acceleration of gravity
H_{m0} = energy-based significant wave height

Figure 3 plots the dimensionless combined wave/surge average overtopping discharge versus the relative (negative) freeboard for all 27 experiments. The indicated surge levels in the plot legend are the average of the negative freeboards determined for all nine experiments at each nominal surge level.

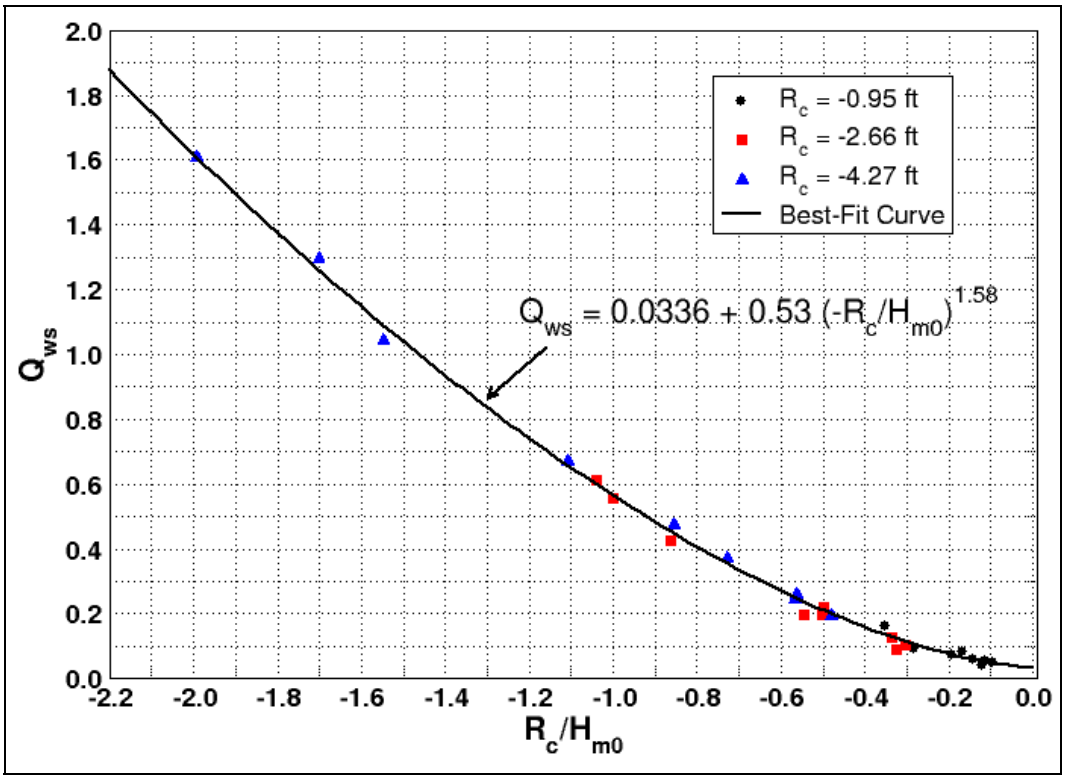

Figure 3. Dimensionless combined wave/surge average discharge versus relative freeboard.

As shown in Figure 3, the measurements gave a nice trend with increasing relative freeboard, and the solid line is a best-fit empirical equation given by the formula

$$Q_{ws} = \frac{q_{ws}}{\sqrt{g\ H_{m0}^3}} = 0.0336 + 0.53\left(\frac{-R_c}{H_{m0}}\right)^{1.58} \quad (2)$$

This best-fit equation had a correlation coefficient of 0.9987 and a root-mean-square (RMS) percent error of 0.12. (Note that R_c must be specified as a negative number so the ratio in brackets will be positive.) Peak spectral wave period had negligible influence in the determination of Q_{ws} for the range of periods tested in the model.

Like any empirical equation, application of Equation 2 should be limited to the range of tested parameters. In particular, seaward (flood-side) levee slopes different from 1:4.25 could influence the wave overtopping, but seaward slope effects should decrease as surge level increases. For zero freeboard ($R_c = 0$), Equation 2 yields a constant dimensionless average wave overtopping rate that falls near the middle of the range of experiment results given by Schüttrumpf et al. (2001). This is encouraging; however, estimates for zero freeboard should be made using Schüttrumpf's equations as presented in the Overtopping Manual (Pullen et al. 2007) rather than Equation 2.

PROBABILITY DISTRIBUTION OF INSTANTANEOUS DISCHARGE: During combined wave and surge overtopping, each wave will have instantaneous peak discharge that can be several times the average overtopping rate, q_{ws}. These peak discharges, while short in duration, may be responsible for much of the erosion of levee soil or instability/failure of armoring alternatives. Thus, prediction of the instantaneous overtopping distribution is needed for more effective design of levee slope protection alternatives.

The time series measurements of overtopping flow discharge acquired near the landward-side edge of the levee crest were analyzed to determine the cumulative distribution of instantaneous discharge over the levee crest. The analysis revealed that still-water elevation above the levee crest (i.e., the steady overflow discharge) is the most important hydrodynamic parameter, and it most closely controls the scale of the cumulative probability distribution. Wave height and period appear to influence the shape of the distribution extreme tail.

The measured cumulative discharge distributions were fit to the Weibull cumulative probability distribution given by the expression

$$P(q \le q_*) = 1 - \exp\left[-\left(\frac{q_*}{c}\right)^b\right] \quad (3)$$

where c is the "scale factor" and b is the "shape factor" of the distribution. The scale factor, c, has units of discharge per unit length, whereas the shape factor, b, is dimensionless. Equation 3 gives the probability that a value of discharge will be below the specified discharge, q_*. The corresponding distribution of percent exceedance is given by

$$P_{\%}(q > q_*) = 100 \cdot \exp\left[-\left(\frac{q_*}{c}\right)^b\right] \quad (4)$$

The best-fit procedure produced values of the distribution parameters, *b* and *c*. Figure 4 shows an example of a good fit (upper plot) and a mediocre fit (lower plot) of the Weibull cumulative distribution to the measured distributions (given as percent exceedance distributions). The curves are plotted with a semi-log ordinate to better present the extreme end of the exceedance probability.

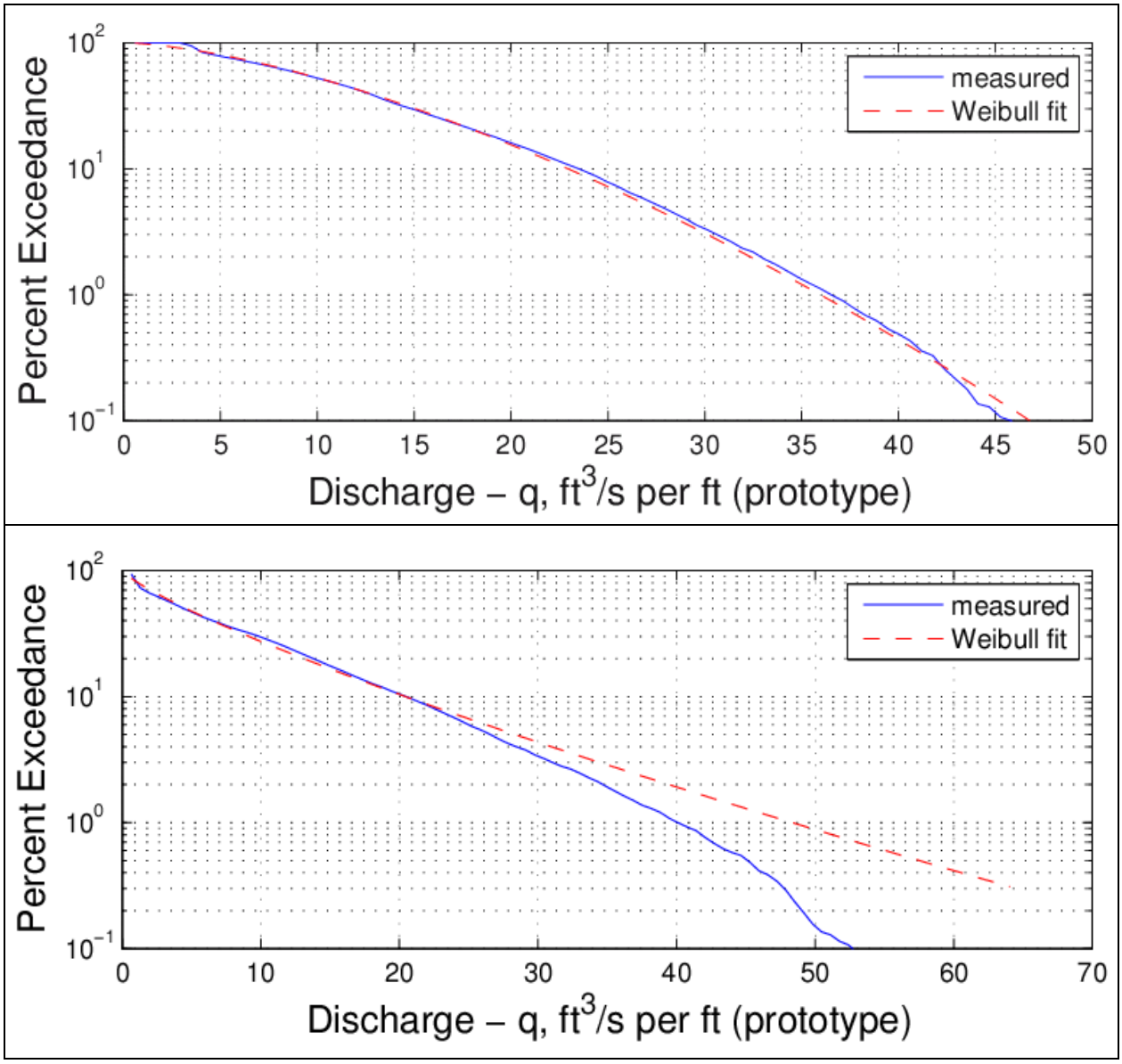

Figure 4. Example best fits of Weibull cumulative probability distribution to instantaneous discharge.

The curves in Figure 4 give the percent occurrence that the overtopping discharge will be *above* a given value. For example, in the upper plot of Figure 4, for 10 percent of the time the discharge will be above $q \approx 23$ ft^3/sec per foot, and the discharge will exceed $q \approx 36$ ft^3/sec per foot for 1 percent of the time. The average wave/surge overtopping for this experiment was $q_{ws} = 13.1$ ft^3/sec per foot.

The dimensionless shape factor, b, exerts control over the extreme tail of the distribution, and the tail is sensitive to small differences in the shape factor. Through inspection, and after several attempts using dimensionless combinations of the wave height, wave period, and steady surge discharge, the best empirical result for the shape factor was the relationship

$$b = 8.10\left(\frac{q_s}{g\,H_{m0}\,T_p}\right)^{0.343} \tag{5}$$

where q_s is estimated from the broad-crest weir formulation as

$$q_s = \left(\frac{2}{3}\right)^{3/2}\sqrt{g}\,|R_c|^{3/2} = 0.5443\sqrt{g}\,|R_c|^{3/2} \tag{6}$$

Figure 5 shows the best-fit curve for the shape factor given by Equation 5 along with the plotted values of b obtained from the measured data. The correlation coefficient for the best fit was 0.922.

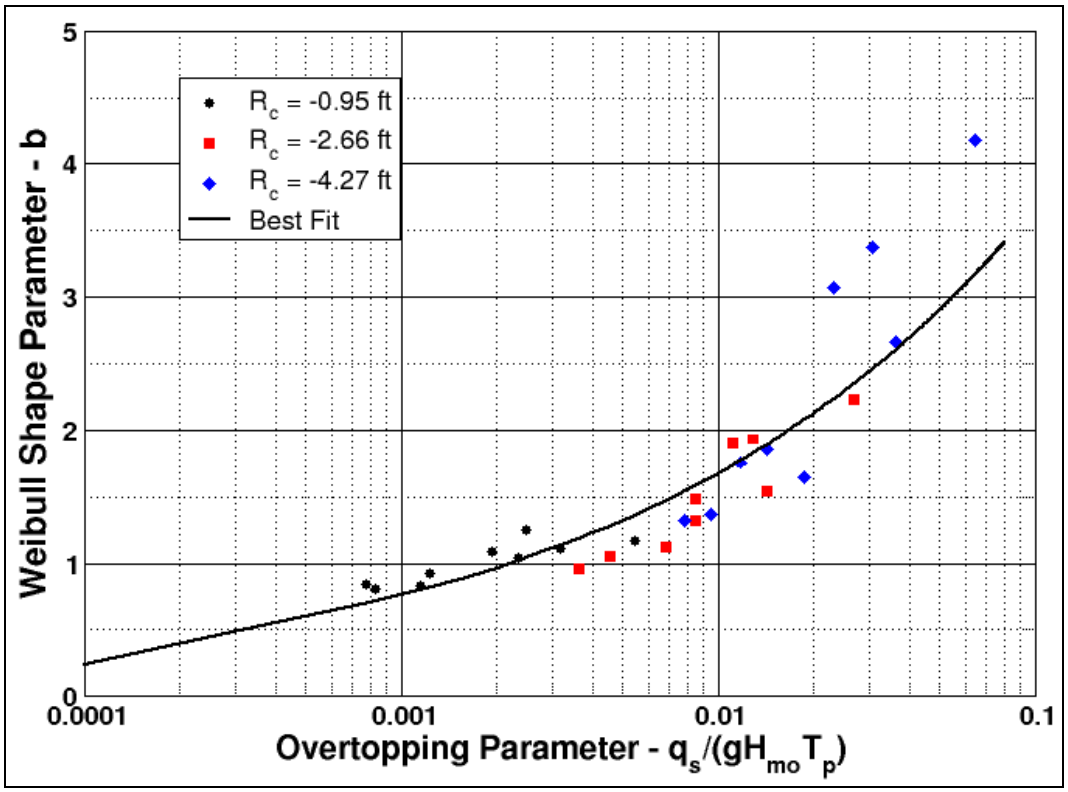

Figure 5. Best-fit equation for Weibull parameter *b*.

The three data points in Figure 5 with values of b greater than 3 deviated significantly from the data trend. These points came from experiments with the surge level at approximately +4.3 ft and nominal wave heights around 3 ft (scaled from model to prototype). A possible explanation for the observed deviation might be the effect of wave deformation by the strong steady overflow as waves reach the levee. The nonlinear interaction between the waves and the coincident current at the levee

crest is more pronounced at the higher surge level, and smaller waves would be affected more than larger waves. The resulting smaller wave heights would reduce the extreme values of overtopping discharge, giving higher values for the shape factor, *b*.

The mean of the Weibull cumulative distribution is equal to the average overtopping discharge, q_{ws}, and it can also be expressed in terms of the *b* and *c* parameters as (e.g., Goda 2000)

$$q_{ws} = c \cdot \Gamma\left(1 + \frac{1}{b}\right) \tag{7}$$

where Γ is the mathematical gamma function. Equation 7 was used to estimate q_{ws} using the best-fit values of the Weibull *b* and *c* parameters for all experiments, and comparison with values of q_{ws} determined directly from the discharge time series showed excellent agreement. Therefore, Equation 7 can be rearranged to give an expression for the scale factor, *c*, i.e.,

$$c = \frac{q_{ws}}{\Gamma\left(1 + \frac{1}{b}\right)} \tag{8}$$

The gamma function can be accurately calculated over the range of shape factor, *b*, found for these experiments ($0.5 < b < 4$) by the best fit of a cubic equation given by

$$\Gamma(x) = 1.3 - 0.368 \cdot x - 0.072 \cdot x^2 + 0.09 \cdot x^3 \tag{9}$$

which is valid for $1.25 < x < 3$. This approximation can be used for calculations when the gamma function is not available.

In summary, the cumulative probability distribution of instantaneous discharge over the levee crest due to combined wave and surge overtopping can be estimated using Equation 3 or 4 with the Weibull shape factor, *b*, determined from Equation 5, and the Weibull scale factor, *c*, estimated using Equation 8 as a function of q_{ws} (from Equation 2). For an application in which calculation of the gamma function is not available, use Equation 9 within the stated range of applicability.

FLOW PARAMETERS ON THE LANDWARD-SIDE LEVEE SLOPE: Steady overflow on the steep landward-side slope of a levee is supercritical with slope-parallel velocities increasing down the slope until a balance is reached between the momentum of the flow and the frictional resistance force of the slope surface. Once terminal velocity is reached (mean velocity is constant), the steady flow can be analyzed using the Chezy or Manning equation. Flow down the landward-side slope caused by combined waves and surge overtopping is unsteady and more difficult to analyze thoroughly. In this section empirical equations are given to characterize several representative parameters of wave-related unsteady flow on the landward-side levee slope.

Average Flow Depth on Landward-Side Slope. The average flow depth, η_m, perpendicular to the slope was calculated at four pressure gauge locations that were equally spaced down the landward-side slope. Comparison among the four gauges indicated the values of η_m were nearly constant for each experiment, so an average was taken to represent the mean flow thickness on the

landward-side slope. A correlation was sought between η_m and the hydrodynamic forcing, and a reasonable result is shown in Figure 6. Values have been scaled to prototype dimensions using a length scale ratio of 25-to-1. The solid line is a linear best-fit equation given by the simple empirical expression

$$\frac{q_{ws}}{\sqrt{g\eta_m^3}} = 2.226 \tag{10}$$

This equation had a correlation coefficient of 0.988, and an RMS percent error of 0.134.

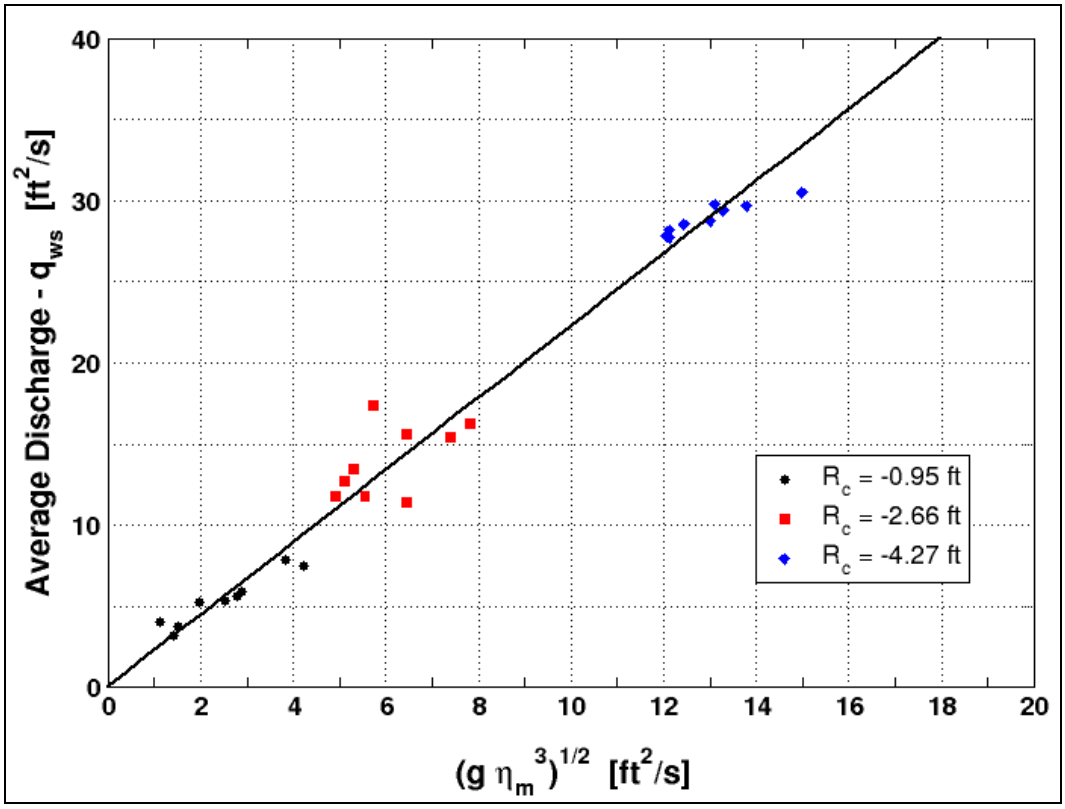

Figure 6. Average overtopping discharge versus mean flow thickness on landward-side slope (prototype scale).

If the mean velocity on the landward-side slope is defined as $v_m = q_{ws} / \eta_m$, then

$$v_m = 2.226\sqrt{g\eta_m} \tag{11}$$

which bears resemblance to the Chezy equation.

The Chezy equation for wide channels (hydraulic radius is approximately equal to flow depth, d) and steady flow (friction slope is equal to landward-side levee slope, θ) is given as

$$v = \sqrt{\frac{2\sin\theta}{f_F}} \cdot \sqrt{g\,d} \tag{12}$$

for steep slopes. In Equation 12 the Chezy coefficient was replaced with a function of the Fanning friction factor given by the expression

$$C_Z = \sqrt{\frac{2g}{f_F}} \tag{13}$$

Under the assumption the Chezy equation is an appropriate model to approximate the average of this rapidly varying unsteady flow situation, it is hypothesized that the constant in Equations 10 and 11 is a function of both levee slope and a representative friction factor, as given by the first radical term in Equation 12.

The Chezy coefficient C_Z varies with flow thickness on the slope; therefore, the friction factor, f_F, also varies continuously during the unsteady overtopping flow. A representative friction factor for these experiments was found by assuming that the constant in Equation 11 is equal to the first radical term in Equation 12. This yielded a value of $f_F = 0.128$. However, at this point there is no method for estimating similar representative friction factors for other slope roughness, so little benefit is gained by including friction factor at this time. It is assumed, however, that the representation of structure slope in Equation 12 is reasonable. For the 1-on-3 slope in these experiments, the constant in Equations 10 and 11 was determined to be $2.226 = 3.96\sqrt{\sin\theta}$.

Substituting for the constant in Equation 10 and rearranging gives a tentative equation for the mean flow depth, i.e.,

$$\eta_m = 0.4 \left[\frac{1}{g\sin\theta}\right]^{1/3} (q_{ws})^{2/3} \tag{14}$$

and the mean flow velocity equation becomes the following

$$v_m = 2.5\,(q_{ws} \cdot g \cdot \sin\theta)^{1/3} \tag{15}$$

The constants in Equations 14 and 15 are related to the slope roughness, and the equations are applicable only for landward-side slopes having roughness similar to that of the laboratory experiments. Friction factors for grass levee slopes should not be too much higher than those of the experiments, but slopes armored with riprap or similar material will have significantly higher representative friction factors. More work is needed to determine appropriate representative friction factors for a range of slope roughness.

Estimation of H_{rms} on the Landward-Side Slope. Values of root-mean-square wave height, H_{rms}, perpendicular to the slope at the four pressure gauge locations on the landward-side slope were averaged based on the observation that little variation was shown over this down-slope distance. A relationship was sought that expressed H_{rms} in terms of other parameters that could be estimated. Figure 7 shows the best correlation of those attempted. Wave period was found to have only

marginal influence, and some of the observed scatter is possibly explained by wave period variation. The solid curve represents the best fit of a one-parameter exponential function given as

$$\frac{H_{rms}}{\eta_m} = 3.43 \cdot \exp\left(\frac{R_c}{H_{m0}}\right) \tag{16}$$

This best-fit equation had a correlation coefficient of 0.966 and an RMS percent error of 0.094. When applying Equation 16, keep in mind that R_c must be entered as a negative number, and the equation should not be applied for cases in which $R_c \geq 0$ (surge level is at or below the crest elevation).

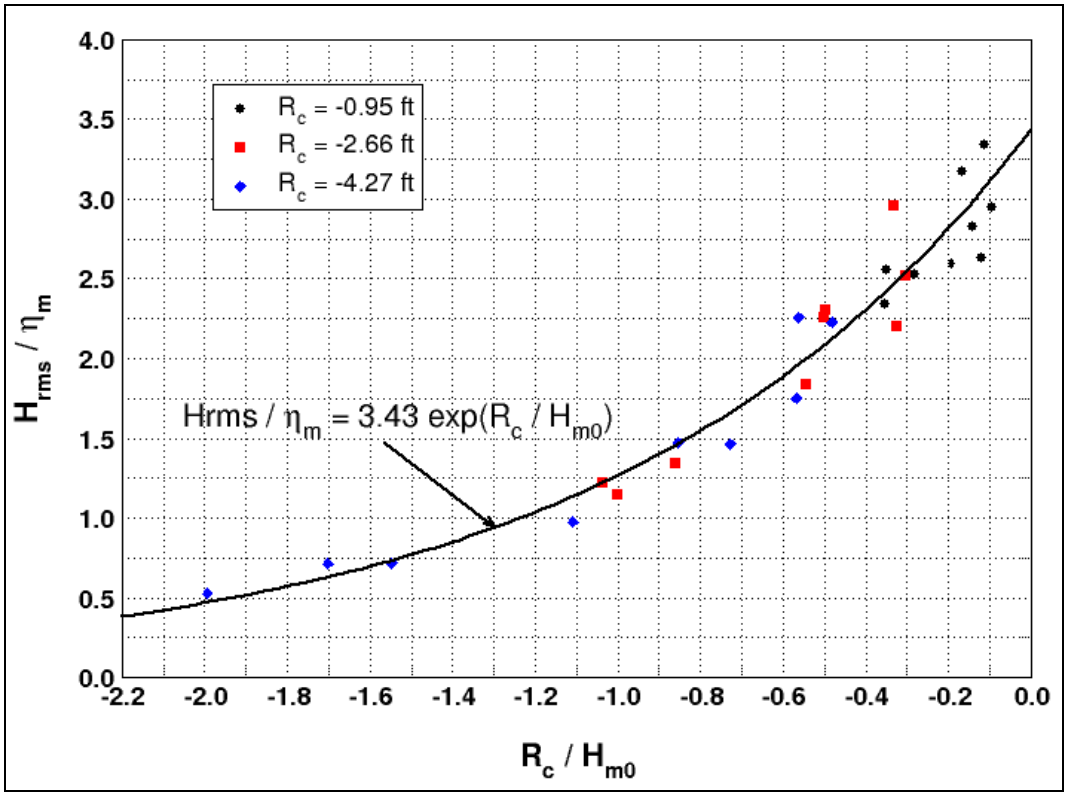

Figure 7. Estimation of H_{rms} on the landward-side slope as a function of η_m.

The effect of levee landward-side slope is included in Equation 16 through the estimation of the mean flow depth, η_m, using Equation 14. However, this is still tentative and may not be correct, so caution is urged until additional verification of Equation 16 is forthcoming. Also, note that H_{rms}/η_m is less than unity when R_c/H_{m0} is less than -1.2. In these cases, the landward-side slope does not go dry during passage of the wave trough, and the mean flow depth is greater than the crest-to-trough length represented by H_{rms}.

Once H_{rms} is estimated, the Rayleigh distribution can be used to obtain reasonable estimates for $H_{1/3}$ and $H_{1/10}$ according to the equations

$$H_{1/3} = 1.416 \cdot H_{rms} \qquad and \qquad H_{1/10} = 1.80 \cdot H_{rms} \tag{17}$$

Comparisons between measured characteristic wave heights and those predicted by the Rayleigh distribution using measured values of H_{rms} were performed for all laboratory data. An excellent prediction was found for $H_{1/3}$, and the prediction for $H_{1/10}$ was quite good with a little more scatter and a tendency to overpredict slightly. However, the Rayleigh distribution overpredicted the measured values of $H_{1/100}$ by as much as 25 to 40 percent, indicating that the highest waves do not conform well to the Rayleigh distribution. Nevertheless, the reasonable fit of the Rayleigh distribution is a useful finding because it allows much of the wave height distribution on the landward-side slope to be characterized in terms of the RMS wave height, H_{rms}.

Estimation of Wave Front Velocity on the Landward-Side Slope. Flow velocity was not measured directly on the landward-side slope during the laboratory experiments. However, it was possible to make a rough estimate of the speed of the wave front by dividing the distance between the first and last pressure gauges by the time it took the wave front to move over that distance. This approximate wave front velocity represents an average over the distance between the four pressure gauges. In fact, the flow might have been accelerating over this reach. The accuracy of wave front velocity estimates using this technique is limited by the data sampling rate of 50 Hz used in the experiments. One data point shift either way is a relatively large change in estimated velocity. For this reason, the wave front velocity analysis was restricted to the first and last gauges to maximize the distance between gauges, and thus, to reduce the potential for error.

Figure 8 plots the wave front velocity versus the velocity of a bore having a frontal depth equal to H_{rms}. Values of H_{rms} were the averages taken over the four pressure gauges. The discrete jumps in velocity on the plot ordinate represent time shifts of four, five, six, and seven time steps (highest to lowest velocity). The actual wave front velocities of some points are probably somewhere between the levels, and this could reduce the scatter somewhat. The straight line shown in Figure 8 is the best fit given by the equation

$$v_w = 3.85 \sqrt{g\, H_{rms}} \tag{18}$$

where v_w is the wave front velocity. This best fit had a correlation coefficient of 0.891 and an RMS percent error of 0.114. The coefficient in Equation 18 is constant for this particular data set; however, it may be a function of slope angle and surface roughness even though Equation 16 for estimating H_{rms} explicitly includes slope and implicitly includes friction effects for smooth slopes.

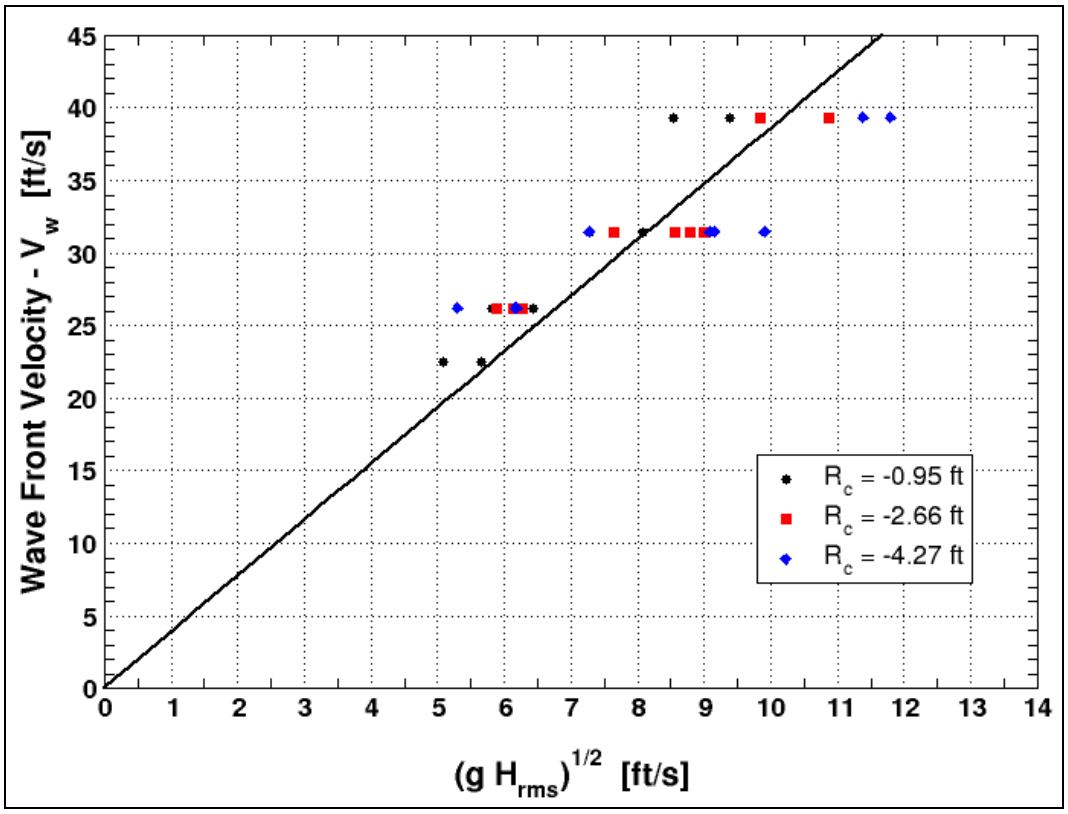

Figure 8. Estimated wave front velocity determined from the first and last pressures gauges.

Example: Combined Wave/Surge Overtopping Flow Parameters

Find: The flow parameters associated with wave overtopping combined with overflow by a surge elevation that is 1.3 ft above the levee crest elevation. The levee surface is considered smooth with roughness comparable to grass or turf reinforcement mats.

Given:

H_{m0}	= 6 ft	=	zeroth-moment significant wave height
T_p	= 8 sec	=	wave period associated with the spectral peak
h_c	= 17.0 ft	=	levee crest elevation
h_S	= 18.3 ft	=	storm surge elevation
R_c	= -1.3 ft	=	freeboard [= h_c - h_S]
tan α	= 1/4	=	seaward-side levee slope
tan θ	= 1/3	=	landward-side levee slope [θ = 18.4 deg]
g	= 32.2 ft/sec^2	=	acceleration due to gravity

The seaward-side levee slope is not used in these calculations, but it is wise to make sure the slope is not too different from the 1-on-4.25 seaward-side slope used in the physical model study on which these equations are based.

Calculate Average Overtopping Discharge. The dimensionless average overtopping discharge is found using Equation 2.

$$Q_{ws} = 0.0336 + 0.53\left(\frac{-R_c}{H_{m0}}\right)^{1.58}$$

$$= 0.0336 + 0.53\left(\frac{-(-1.3\,\text{ft})}{6\,\text{ft}}\right)^{1.58}$$

$$Q_{ws} = 0.081$$

And, the dimensional overtopping is calculated by rearranging Equation 1 to yield

$$q_{ws} = \sqrt{g\,H_{m0}^3}\;Q_{ws} = \sqrt{(32.2\,\text{ft/sec}^2)(6\,\text{ft}^3)}\cdot 0.081$$

$$q_{ws} = 6.75\,\text{ft}^2/\text{sec}$$

(Note the discharge units square feet per sec are equivalent to cubic feet per sec per foot, or cfs/ft.)

Calculate Instantaneous Overtopping Discharge Cumulative Distribution. The Weibull percent exceedance cumulative probability distribution is given by Equation 4. The first step in determining the distribution parameters is estimating the steady overflow discharge (Equation 6) due to the surge elevation exceeding the crest elevation.

$$q_s = 0.5443\sqrt{g}\,\left|R_c\right|^{3/2} = 0.5443\sqrt{32.2\,\text{ft/sec}^2}\,\left|-1.3\,\text{ft}\right|^{3/2}$$

$$q_s = 4.58\,\text{ft}^2/\text{sec}$$

(Note that $q_{ws}/q_s = 1.47$.) Now, calculate the Weibull distribution shape factor, b, using Equation 5.

$$b = 8.10\left(\frac{q_s}{g\,H_{m0}\,T_p}\right)^{0.343} = 8.10\left(\frac{4.58\,\text{ft}^2/\text{sec}}{(32.2\,\text{ft/sec}^2)(6\,\text{ft})(8\,\text{sec})}\right)^{0.343} = 1.1$$

The Weibull scale factor, c, is given by Equation 8. For convenience, evaluate the gamma function in Equation 8 using Equation 9 with $x = 1 + 1/b = 1.91$, i.e.,

$$\Gamma(x) = 1.3 - 0.368\cdot x - 0.072\cdot x^2 + 0.09\cdot x^3$$

$$\Gamma(1.91) = 1.3 - 0.368\cdot(1.91) - 0.072\cdot(1.91)^2 + 0.09\cdot(1.91)^3$$

$$\Gamma(1.91) = 0.962$$

Substituting for the gamma function in Equation 8 yields

$$c = \frac{q_{ws}}{\Gamma\left(1+\frac{1}{b}\right)} = \frac{6.75\,\text{ft}^2/\text{sec}}{\Gamma\left(1+\frac{1}{1.1}\right)} = \frac{6.75\,\text{ft}^2/\text{sec}}{0.962} = 7.02\,\text{ft}^2/\text{sec}$$

The percent exceedance cumulative probability distribution for this example becomes

$$P_{\%}(q > q_*) = 100 \cdot \exp\left[-\left(\frac{q_*}{7.02\,\text{ft}^2/\text{sec}}\right)^{1.1}\right]$$

As an example, the percentage of instantaneous overtopping discharge exceeding $q_* = 15$ cfc/ft is given by

$$P_{\%}(q > 15\,\text{ft}^2/\text{sec}) = 100 \cdot \exp\left[-\left(\frac{15\,\text{ft}^2/\text{sec}}{7.02\,\text{ft}^2/\text{sec}}\right)^{1.1}\right] = 10.0\%$$

In other words, 10 percent of the instantaneous discharge values are greater than 2.2 times the average overtopping discharge.

Calculate Flow Parameters on the Landward-Side Levee Slope. Under the assumption that the levee surface roughness is small (similar to the smooth slope used in the laboratory tests), the mean flow thickness perpendicular to the landward-side slope is estimated from Equation 14 as

$$\eta_m = 0.4\left[\frac{1}{g\sin\theta}\right]^{1/3}(q_{ws})^{2/3} = 0.4\left[\frac{1}{(32.2\,\text{ft/sec}^2)\sin(18.4^o)}\right]^{1/3}(6.75\,\text{ft}^2/\text{sec})^{2/3}$$

$$\eta_m = 0.4\left(0.462\,\text{s}^{2/3}/\text{ft}^{1/3}\right)\left(3.572\,\text{ft}^{4/3}/\text{s}^{2/3}\right) = 0.66\,\text{ft}$$

The mean flow velocity on the landward-side slope can be estimated using Equation 15, but an easier method is using the definition

$$v_m = \frac{q_{ws}}{\eta_m} = \frac{6.75\,\text{ft}^2/\text{sec}}{0.66\,\text{ft}} = 10.2\,\text{ft/sec}$$

The RMS wave height (perpendicular to the levee slope) is estimated from Equation 16 as

$$H_{rms} = \eta_m\left[3.43 \cdot \exp\left(\frac{R_c}{H_{m0}}\right)\right] = (0.66\,\text{ft})\left[3.43 \cdot \exp\left(\frac{-1.3\,\text{ft}}{6\,\text{ft}}\right)\right]$$

$$H_{rms} = 1.8\,\text{ft}$$

Because the wave heights on the landward-side slope appear to follow the Rayleigh distribution except at the extreme tail, other representative wave heights can be estimated from Equation 17, i.e.,

$$H_{1/3} = 1.416 \cdot H_{rms} = 1.416 \cdot (1.8\,\text{ft}) = 2.6\,\text{ft}$$

$$H_{1/10} = 1.80 \cdot H_{rms} = 1.80 \cdot (1.8\,\text{ft}) = 3.2\,\text{ft}$$

Finally, a rough estimate of the velocity of the overtopping wave front on the landward-side slope is given by Equation 18 as

$$v_w = 3.85\sqrt{g\,H_{rms}} = 3.85\sqrt{(32.2\,\text{ft/sec}^2)(1.8\,\text{ft})}$$
$$v_w = 29.3\,\text{ft/sec}$$

The velocity of the wave front is almost 3 times greater than the mean velocity on the landward-side slope. Most importantly, the wave front velocity estimate should be considered preliminary, and the margin for error is significant due to the method by which the equation was developed.

Flow Parameter Variation for Same Average Overtopping Discharge. Different combinations of incident wave height and freeboard can produce the same value of average overtopping discharge, q_{ws}. Table 1 shows overtopping flow parameters calculated for three additional cases that produced the same average discharge (q_{ws} = 6.75 ft^2/sec) determined above.

Table 1
Additional Parameter Estimates for the Same Value of q_{ws}

H_{m0} (ft)	R_c (ft)	q_{ws} (ft^2/sec)	q_s (ft^2/sec)	b	c (ft^2/sec)	η_m (ft)	v_m (ft/sec)	H_{rms} (ft)	v_w (ft/sec)
1.0	-1.64	6.75	6.49	2.3	7.60	0.66	10.2	0.44	14.5
3.0	-1.59	6.75	6.22	1.5	7.50	0.66	10.2	1.33	25.2
6.0	-1.30	6.75	4.58	1.1	7.02	0.66	10.2	1.80	29.3
9.0	-0.75	6.75	2.00	0.7	5.46	0.66	10.2	2.08	31.5

REMARKS: All four of the cases given in the table above have different combinations of incident significant wave height and levee freeboard, although the average overtopping discharge, q_{ws}, was the same. The mean flow parameters on the landward-side slope (η_m and v_m) were also identical. However, the parameters of the Weibull distribution of instantaneous discharge (b and c), the RMS wave height (H_{rms}), and the velocity of the wave front (v_w) were quite different among the cases. The difference of wave height and wave front velocity on the landward-side slope suggests that characterizing levee safety in terms of an upper limit for average overtopping discharge may not be prudent unless it can be shown that levee erosion and armor stability is more a function of the mean flow characteristics than a function of the variations in the unsteady overtopping flow.

SUMMARY: This CHETN summarized new equations for average overtopping discharge and distribution of instantaneous discharge associated with combined wave and storm surge overtopping of levees. Equations are also given for mean flow thickness, RMS wave height, mean velocity, and

velocity of the wave front down the landward-side slope. An example problem illustrates application of the new equations. These equations are intended for use in preliminary design.

The empirical equations are based on small-scale laboratory experiments featuring a levee with a seaward-side slope of 1:4.25, and the equations may not be applicable for levees having different seaward-side slopes. It is hypothesized that seaward-side slope may not be as important for combined wave and surge overtopping as it is for wave-only overtopping. Additionally, several assumptions were invoked during equation development. First, it was assumed that unsteady overtopping flow velocities over the levee crest are horizontal and uniform throughout the depth at each instant in time. Second, the equations for the landward-side slope include slope angle and a constant that is likely a function of some representative friction factor characterizing slope roughness. Applicability of these equations for landward-side slopes different from 1-on-3 is uncertain, and the equations will give incorrect estimates where slope surface roughness is not relatively smooth. Finally, the flows down the landward-side slope in the small-scale experiments had little if any air entrainment. This is certainly not the case for similar flows at full scale. How this aeration scale effect alters the parameters estimated by the empirical equations is not yet known.

ADDITIONAL INFORMATION: This CHETN is a product of the Affordable Levee Strengthening and New Design Work Unit being conducted at the U.S. Army Engineer Research and Development Center, Coastal and Hydraulics Laboratory, and sponsored by the Department of Homeland Security Levee Strengthening and Damage Mitigation Program. Questions about this technical note can be addressed to Dr. Steven A. Hughes (Voice: 601-634-2026, Fax: 601-634-3433, email: Steven.A.Hughes@usace.army.mil). Beneficial reviews were provided by Norberto C. Nadal and William C. Seabergh. This document should be cited as:

> Hughes, S. A. 2008. *Estimation of combined wave and storm surge overtopping at earthen levees*. Coastal and Hydraulics Engineering Technical Note ERDC/CHL CHETN-III-78. Vicksburg, MS: U.S. Army Engineer Research and Development Center. *http://chl.erdc.usace.army.mil/chetn*.

REFERENCES

Goda, Y. 2000. *Random seas and design of maritime structures*. 2d ed. Singapore: World Scientific Publishing.

Pullen, T., N.W.H. Allsop, T. Bruce, A. Kortenhaus, H. Schüttrumpf, and J. W. van der Meer. 2007. EurOtop—wave overtopping of sea defences and related structures: Assessment manual. *www.overtopping-manual.com*.

Schüttrumpf, H., J. Möller, H. Oumeraci, J. Grüne, and R. Weissmann. 2001. Effects of natural sea states on wave overtopping of seadikes. *Proceedings of the 4th International Symposium Waves 2001, Ocean Wave Measurement and Analysis*. American Society of Civil Engineers, 2:1565-1574.